ENERGY-BASED MODELS FOR CONTINUAL LEARNING

Shuang Li MIT CSAIL lishuang@mit.edu Yilun Du MIT CSAIL yilundu@mit.edu Gido M. van de Ven Baylor College of Medicine ven@bcm.edu

Antonio Torralba MIT CSAIL torralba@mit.edu Igor Mordatch
Google
imordatch@google.com

ABSTRACT

We motivate Energy-Based Models (EBMs) as a promising model class for continual learning problems. Instead of tackling continual learning via the use of external memory, growing models, or regularization, EBMs have a natural way to support a dynamically-growing number of tasks or classes that causes less interference with previously learned information. We find that EBMs outperform the baseline methods by a large margin on several continual learning benchmarks. We also show that EBMs are adaptable to a more general continual learning setting where the data distribution changes without the notion of explicitly delineated tasks. These observations point towards EBMs as a class of models naturally inclined towards the continual learning regime.

1 Introduction

Humans are able to rapidly learn new skills and continuously integrate them with prior knowledge. The field of Continual Learning (CL) seeks to build artificial agents with the same capabilities (Parisi et al., 2019). In recent years, continual learning has seen increased attention, particularly in the context of classification problems. A crucial characteristic of continual learning is the ability to learn new data without forgetting prior data. Models must also be able to incrementally learn new skills, without necessarily having a notion of an explicit task identity. However, standard neural networks (He et al., 2016; Simonyan & Zisserman, 2014; Szegedy et al., 2015) experience the catastrophic forgetting problem and perform poorly in this setting. Different approaches have been proposed to mitigate catastrophic forgetting, but many rely on the usage of external memory (Lopez-Paz & Ranzato, 2017; Li & Hoiem, 2017), additional models (Shin et al., 2017), or auxiliary objectives and regularization (Kirkpatrick et al., 2017; Schwarz et al., 2018; Zenke et al., 2017; Maltoni & Lomonaco, 2019), which can constrain the wide applicability of these methods.

In this work, we focus on classification tasks. These tasks are usually tackled by utilizing normalized probability distribution (i.e., softmax output layer) and trained with a cross-entropy objective. In this paper, we argue that by viewing classification from the lens of training an un-normalized probability distribution, we can significantly improve continual learning performance in classification problems. In particular, we interpret classification as learning an Energy-Based Model (EBM) across seperate classes. Training becomes a wake-sleep process, where the energy of an input data at its ground truth label is decreased while the energy of the input at (an)other selected class(es) is increased. An important advantage is that this framework offers freedom to choose what classes to update in the continual learning process. By contrast, the cross entropy objective reduces the likelihood of *all* negative classes when given a new input, creating updates that lead to catastrophic forgetting.

The energy function, which maps an input-label pair to a scalar energy, also provides a way for the model to select and filter portions of the input that are relevant towards the classification on hand. We show that this enables EBMs training updates for new data to interfere less with previous data. In particular, our formulation of the energy function allows us to compute the energy of an input by learning a conditional gain based on the class label, which serves as an attention filter to select the most relevant information. In the event of a new class, a new conditional gain can be learned.

These unique properties benefit EBMs in addressing two important open challenges in continual learning. 1) Firstly, we show that EBMs are very promising for class-incremental learning, which is one of the most challenging settings for continual learning (van de Ven & Tolias, 2019). Successful existing methods for class-incremental learning either store data or use generative replay, which has disadvantages in terms of memory and/or computational efficiency. We show that EBMs perform well in class-incremental learning without using replay and without relying on stored data. 2) The second open challenge that EBMs can address is continual learning without task boundaries. Typically, a continual learning problem is set up as a sequence of distinct tasks with clear boundaries that are known to the model (the *boundary-aware* setting). Most existing continual learning methods rely on these known boundaries for performing certain consolidation steps (e.g., calculating parameter importance, updating a stored copy of the model). However, assuming such clear boundaries is not always realistic, and often a more natural scenario is the *boundary-agnostic* setting (Zeno et al., 2018; Rajasegaran et al., 2020), in which data distributions gradually change without a clear notion of task boundaries. While many common CL methods cannot be used without clear task boundaries, we show that EBMs can be naturally applied to this more challenging setting.

There are four primary contributions of our work. First, we introduce energy-based models (EBMs) for classification continual learning problems. We show that EBMs can naturally deal with challenging problems in CL, including the boundary-agnostic setting and class-incremental learning without using replay. Secondly, we use a contrastive divergence training procedure and we show that it provides a natural way to dynamically grow the number of classes and that it significantly reduces catastrophic forgetting. Thirdly, we propose to learn new conditional gains during the training process, which makes EBMs parameter updates cause less interference with old data. Lastly, we show that in practice EBMs bring a significant improvement on four standard CL benchmarks: split MNIST, permuted MNIST, CIFAR-10, and CIFAR-100. These observations point towards EBMs as a class of models naturally inclined towards the CL regime and as an important baseline upon which to build further developments. The code are made public to facilitate further research ¹.

2 Related work

2.1 CONTINUAL LEARNING SETTINGS

Boundary-aware versus boundary-agnostic. In most existing continual learning studies, models are trained in a "boundary-aware" setting, in which a sequence of distinct tasks with clear task boundaries is given (e.g., Kirkpatrick et al., 2017; Zenke et al., 2017; Shin et al., 2017). Typically there are no overlapping classes between any two tasks; for example task 1 has data with ground truth class labels "1,2" and task 2 has data with ground truth class labels "3,4". In this setting, models are first trained on the entire first task and then move to the second one. Moreover, models are typically told when there is a transition from one task to the next. However, it could be argued that it is more realistic for tasks to change gradually and for models to not be explicitly informed about the task boundaries. Such a boundary-agnostic setting has been explored in (Zeno et al., 2018; Rajasegaran et al., 2020; Aljundi et al., 2019). In this setting, models learn in a streaming fashion and the data distributions gradually change over time. For example, the percentage of "1s" presented to the model might gradually decrease while the percentage of "2s" increases. Importantly, most existing continual learning approaches are not applicable to the boundary-agnostic setting as they require the task boundaries to decide when to consolidate the knowledge (Zeno et al., 2018). In this paper, we will show that our proposed approach can also be applied to the boundary-agnostic setting.

Task-incremental versus class-incremental learning. Another important distinction in continual learning is between task-incremental learning and class-incremental learning (van de Ven & Tolias, 2019; Prabhu et al., 2020). In task-incremental learning, also referred to as the multi-head setting (Farquhar & Gal, 2018), models have to predict the label of an input data by choosing only from the labels in the task where the data come from. On the other hand, in class-incremental learning, also referred to as the single-head setting, models have to chose between the classes from all tasks so far when asked to predict the label of an input data. Class-incremental learning is substantially more challenging than task-incremental learning, as it requires models to select the correct labels from the mixture of new and old classes. So far, only methods that store data or use replay have been shown to perform well in the class-incremental learning scenario (Rebuffi et al., 2017; Rajasegaran et al., 2019). In this paper, we try to tackle class-incremental learning without storing data or replay.

¹Code and documentation are available at https://github.com/ShuangLI59/ebm-continual-learning.git

2.2 CONTINUAL LEARNING APPROACHES

In recent years, numerous methods have been proposed to address the catastrophic forgetting problem in continual learning. Here we broadly partition these methods into three categories: taskspecific, regularization, and replay-based approaches.

Task-specific methods. One way to reduce interference between tasks is by using different parts of a neural network for different problems. For a fixed-size network, such specialization could be achieved by learning a separate mask for each task (Fernando et al., 2017; Serra et al., 2018), by *a priori* defining a different, random mask for every task to be learned (Masse et al., 2018) or by using a different set of parameters for each task (Zeng et al., 2019; Hu et al., 2019). Other methods let a neural network grow or recruit new resources when it encounters new tasks, examples of which are progressive neural networks (Rusu et al., 2016) and dynamically expandable networks (Yoon et al., 2017). Although these task-specific approaches are generally successful in reducing catastrophic forgetting, an important disadvantage is that they require knowledge of the task identity at both training and test time. These methods are therefore not suitable for class-incremental learning.

Regularization-based methods. Regularization is used in continual learning to encourage stability of those aspects of the network that are important for previously learned tasks. A popular strategy is to add a regularization loss to penalise changes to model parameters that are important for previous tasks. For example, elastic weight consolidation (EWC) (Kirkpatrick et al., 2017)) and online EWC (Schwarz et al., 2018) evaluate the importance of each parameter using the diagonal elements in the fisher information matrices, while synaptic intelligence (SI) (Zenke et al., 2017) tracks the past and current parameters and estimates their importance online. An alternative strategy is to regularize the network at the functional level. An example of such a method is Learning without Forgetting (Li & Hoiem, 2017), which uses knowledge distillation to encourage stability of the network's learned input-output mapping. Although these regularization-based approaches can be computationally efficient, a disadvantage is that typically they gradually reduce the model's capacity for learning new tasks. Moreover, while in theory regularization-based methods can be used for class-incremental learning, in practice they have been shown to consistently fail on such problems (Farquhar & Gal, 2018; van de Ven & Tolias, 2019).

Replay methods. To preserve knowledge, replay methods periodically rehearse previously acquired information during training (Robins, 1995). One way to do this, referred to as exact or experience replay, is to store data from previous tasks and revisit them when training on a new task. Although this might seem straightforward, critical non-trivial questions are how to select the data to be stored as well as exactly how to use them (Rebuffi et al., 2017; Lopez-Paz & Ranzato, 2017; Rajasegaran et al., 2019; Hou et al., 2019; Wu et al., 2019; Mundt et al., 2020). An alternative to storing data is to generate the data to be replayed. In such generative replay (Shin et al., 2017), a generative model is sequentially trained to generate input samples representative of those from previously seen tasks. While both types of replay can prevent catastrophic forgetting in both task- and class-incremental learning settings, an important disadvantage is that these methods are computationally relatively expensive as each replay event requires at least one forward and one backward pass through the model. In addition, storing data might not always be possible while incrementally training a generative model is a challenging problem in itself (Lesort et al., 2019; van de Ven et al., 2020).

In contrast, our EBMs reduce catastrophic forgetting without requiring knowledge of task-identity, without gradually restricting the model's learning capabilities and without using stored data.

3 CONTINUAL LEARNING WITH SOFTMAX-BASED CLASSIFIERS

By far the most common way to do classification with deep neural networks is to use a softmax output layer in combination with a cross-entropy loss. Similarly, in the continual learning literature, virtually all existing methods for classification are based on the softmax-based classifier (SBC). In this section we start by formally describing classification with a softmax-based classifier. We then describe the challenges of softmax-based classification in the continual learning setting.

3.1 SOFTMAX-BASED CLASSIFICATION

Given an input $\mathbf{x} \in \mathbb{R}^D$ and a discrete set $\mathcal{Y} = \{1, \dots, N\}$ of N possible class labels, a traditional softmax-based classifier defines the conditional probabilities of those labels as:

$$p_{\theta}(y|\mathbf{x}) = \frac{\exp([f_{\theta}(\mathbf{x})]_y)}{\sum_{i \in \mathcal{Y}} \exp([f_{\theta}(\mathbf{x})]_i)}, \text{ for all } y \in \mathcal{Y},$$
 (1)

where $f_{\theta}(\mathbf{x}): \mathbb{R}^D \to \mathbb{R}^N$ is a feed-forward neural network, parameterized by θ , that maps an input \mathbf{x} to a N-dimensional vector of logits. In the above notation, $[\cdot]_i$ indicates the i^{th} element of a vector.

Training. A softmax-based classifier is typically trained by optimizing the cross-entropy loss function. For a given input x and corresponding ground truth label y^+ , the cross-entropy loss is:

$$\mathcal{L}_{CE}(\boldsymbol{\theta}; \mathbf{x}, y^{+}) = -\log(p_{\boldsymbol{\theta}}(y^{+}|\mathbf{x})), \tag{2}$$

Inference. Given an input x, the class label predicted by the softmax-based classifier is the class with the largest conditional probability:

$$\hat{y} = \underset{y \in \mathcal{Y}}{\arg \max} p_{\theta}(y|\mathbf{x}). \tag{3}$$

3.2 SOFTMAX-BASED CLASSIFIERS FOR CONTINUAL LEARNING

When used for continual learning, and in particular when used for class-incremental learning, softmax-based classifiers face several challenges. One important issue is that softmax-based classifiers compute the cross-entropy loss over all classes (or sometimes over all classes that have been seen so far). As a result, when training on a new task, the likelihood of the currently observed classes is increased, but the likelihood of old classes is too heavily suppressed since they are not encountered in the new task. The softmax operation introduces competitive, winner-take-all dynamics that make the classifier catastrophically forget past tasks.

4 CONTINUAL LEARNING WITH ENERGY-BASED MODELS

In section 4.1 we introduce energy-based models (EBMs) and in section 4.2 we describe how EBMs can be used for classification. In sections 4.3.1 and 4.3.2 we highlight two main differences between softmax-based classifiers and energy-based classifiers, which will later be shown to be responsible for the stronger continual learning performance of our EBMs.

4.1 ENERGY-BASED MODELS

EBMs (LeCun et al., 2006) are a class of maximum likelihood models that define the likelihood of a data point $\mathbf{x} \in \mathcal{X} \subseteq \mathbb{R}^D$ using the Boltzmann distribution:

$$p_{\theta}(\mathbf{x}) = \frac{\exp(-E_{\theta}(\mathbf{x}))}{Z(\theta)}, \quad Z(\theta) = \int_{\mathbf{x} \in \mathcal{X}} \exp(-E_{\theta}(\mathbf{x}))$$
 (4)

where $E_{\theta}(\mathbf{x}) : \mathbb{R}^D \to \mathbb{R}$, known as the energy function, maps each data point \mathbf{x} to a scalar energy value, and $Z(\theta)$ is the partition function. In deep learning applications of EBMs, the energy function E_{θ} is a neural network parameterized by θ .

EBMs are powerful models that have been applied to different domains, such as structured prediction (Belanger & McCallum, 2016; Gygli et al., 2017; Rooshenas et al., 2019; Tu & Gimpel, 2019), machine translation (Tu et al., 2020), text generation (Deng et al., 2020), reinforcement learning (Haarnoja et al., 2017; Du et al., 2019), image generation (Salakhutdinov & Hinton, 2009; Xie et al., 2016; 2018; Grathwohl et al., 2019), memory modeling (Bartunov et al., 2019), biologically-plausible training (Scellier & Bengio, 2017), and protein design and folding (Ingraham et al., 2019).

Belanger & McCallum (2016) introduce energy networks for structured prediction. They propose energy networks can be naturally posed as structured prediction, since the labels exhibit rich interaction structure. Tu & Gimpel (2019) propose a structured energy function for sequence labeling tasks. Rooshenas et al. (2019) introduce a search-guided approach to obtain training pairs using a combination of the energy function and reward function that allows the lightly-supervised training of structured prediction energy networks. Tu et al. (2020) treat the non-autoregressive translation system as an inference network that finds the translation by minimizing the energy of a pretrained autoregressive model. Xie et al. (2016) is the first paper to use ConvNet-parameterized EBMs with Langevin dynamics for image generation. They show that a generative random field model can be derived from the commonly used discriminative ConvNet. Xie et al. (2018) cooperatively train the descriptor and generator using MCMC sampling. As far as we are aware, the use of EBMs for continual learning has so far remained unexplored.

4.2 Energy-based models for classification

Here we slightly adapt the above general formulation of an EBM to make it suitable for classification. Given inputs $\mathbf{x} \in \mathbb{R}^D$ and a discrete set \mathcal{Y} of possible class labels, we propose to use the Boltzmann distribution to define the conditional likelihood of label y given \mathbf{x} :

$$p_{\theta}(y|\mathbf{x}) = \frac{\exp(-E_{\theta}(\mathbf{x}, y))}{Z(\theta; \mathbf{x})}, \quad Z(\theta; \mathbf{x}) = \sum_{y \in \mathcal{Y}} \exp(-E_{\theta}(\mathbf{x}, y))$$
 (5)

where $E_{\theta}(\mathbf{x}, y) : (\mathbb{R}^D, \mathbb{N}) \to \mathbb{R}$ is the energy function that maps an input-label pair (\mathbf{x}, y) to a scalar energy value, and $Z(\theta; \mathbf{x})$ is the partition function that ensures $\sum_{y \in \mathcal{Y}} p_{\theta}(y|\mathbf{x}) = 1$ for any given \mathbf{x} .

Training. Inspired by the contrastive divergence proposed by Hinton (2002), we minimize the energy of x at the ground truth label y^+ while increasing the energy of x at other labels. To do so, we use the following per-sample loss:

$$\mathcal{L}_{CD}(\boldsymbol{\theta}; \mathbf{x}, y^{+}) = E_{\boldsymbol{\theta}}(\mathbf{x}, y^{+}) + \log \sum_{y \in \{\mathcal{N}, y^{+}\}} \exp(-E_{\boldsymbol{\theta}}(\mathbf{x}, y)).$$
 (6)

whereby \mathcal{N} is the set of 'negative samples'. See section 4.3.1 for a discussion of how to select these negative samples for continual learning.

Inference. Given an input x, the class label predicted by our energy-based classifier is the class with the smallest energy at x:

$$\hat{y} = \arg\min_{y \in \mathcal{Y}} E_{\theta}(\mathbf{x}, y), \tag{7}$$

4.3 ENERGY-BASED MODELS FOR CONTINUAL LEARNING

4.3.1 SELECTION OF NEGATIVE SAMPLES

A first key difference between our EBM and the softmax-based classifier is the introduction of negative samples. The use of negative samples in the training objective provides freedom for the EBM in the choice of which class labels to train on. This is important because an important issue with softmax-based classifier models is that they suppress old classes too much because the softmax-operation normalizes over all classes.

An important decision is thus how to select the set of negative samples $\mathcal N$ in Equation 6. Following common practice in contrastive divergence, we sample the set of negative classes $\mathcal N$ from the set of class labels in the current batch Y_B , using only a single negative class per training sample. We note however that it is possible to use different strategies for choosing the negative classes, and in the experiments reported in Table 2 we explore alternative strategies: 1) using all classes in the current batch as negative classes (i.e., $\mathcal N=Y_B$); 2) using all classes seen so far as negative classes.

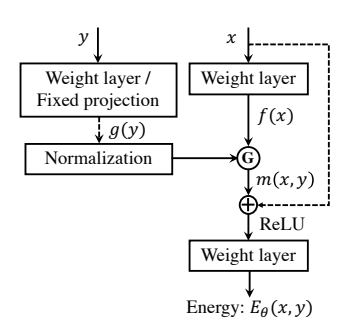


Figure 1: Model architecture used in EBM. EBM takes a data \mathbf{x} and a class y as input and outputs their energy value. The dash lines are optional on different datasets.

Different from the softmax-based classifier, EBMs define the probability without normalizing over all classes but instead sampling a single negative class from the current training batch. This operation cause less interference with previous classes without using any extra information which contributes to why EBMs suffer less from catastrophic forgetting.

Importantly, since we select the negative sample(s) from the current batch, our EBMs do not require knowledge of the task on hand. This allows application of our EBMs in the *boundary-agnostic* continual learning setting, in which the underlying tasks or task boundaries are not given. More broadly speaking, EBMs can go out of the scope of classification problems, and similar ideas can be applied to regression (Gustafsson et al., 2020), generation (Xie et al., 2016; Du et al., 2020), and reinforcement learning (Parshakova et al., 2019), although we do not explore them in this work.

4.3.2 Energy network

Another important difference is that the choice of model architectures also becomes more flexible in EBMs. The traditional classification models can only feed in $\mathbf x$ as input and the classification results only depend on the neural network trained on the current data $\mathbf x$. Thus the models usually fail on the old data after updating network parameters trained on the new data. In contrast, EBMs have many different ways to combine $\mathbf x$ and y in the energy function $E_{\theta}(\mathbf x,y)$ with the only requirement that $E_{\theta}(\mathbf x,y):(\mathbb R^D,\mathbb N)\to\mathbb R$. In EBMs, we can treat y as an attention filter or gate to select the most relevant information between $\mathbf x$ and y.

To compute the energy of any data $\mathbf x$ and class label y pair, we use y to influence a conditional gain on $\mathbf x$, which serves as an attention filter (Xu et al., 2015) to select the most relevant information between $\mathbf x$ and y. In Figure 1, we first send $\mathbf x$ into a small network to generate the feature $f(\mathbf x)$. The label y is mapped into a same dimension feature space g(y) using a FC layer or a random projection. We use the gating block G to select the most relevant information between $\mathbf x$ and y:

$$m(\mathbf{x}, y) = G(f(\mathbf{x}), g(y)). \tag{8}$$

The gating block can be applied several times. The output is finally sent to a fully connected layer to generate the energy value $E_{\theta}(\mathbf{x}, y)$. See Appendix B for more details.

Our EBMs allow any number of classes in new batches by simply training or defining a new conditional gain g(y) for the new classes and generating its energy value with data point x. This formulation gives us freedom to learn new classes without pre-defining their number in advance. We note that the standard classifiers have to change their model architecture by adding new class heads to the softmax output layer when dealing with new classes. In contrast, EBMs do not need to modify the model architecture or resize the network when adding new classes.

4.3.3 Inference

During inference, because we evaluate according to the class-incremental learning scenario (van de Ven & Tolias, 2019; Tao et al., 2020a; He et al., 2018; Tao et al., 2020b), the model must predict a class label by choosing from all classes seen so far. Let \mathbf{x}_k be one data point from a batch B_k with an associated discrete label $y \in Y_k$, where Y_k contains the class labels in B_k . Then there are $Y = \bigcup_{k=1}^K Y_k$ different class labels in total after seeing all the batches. The MAP estimate is

$$\hat{y} = \arg\min_{y} E_{\theta_K}(\mathbf{x}_k, y), \quad y \in \bigcup Y_k, \tag{9}$$

where $E_{\theta_K}(\mathbf{x}_k, y)$ is the energy function with parameters θ_K resulting from training on the batches $\{B_1, \dots, B_K\}$. The energy function can compute an energy for any discrete class input, including unseen classes, which avoids needing to predefine the number of classes in advance.

5 EXPERIMENTS

In this section, we want to answer the following questions: How do the proposed EBMs perform on different CL settings? Can we qualitatively understand the differences between our EBMs and the baselines? Is the proposed EBM training objective with negative samples better than other objectives? Can we apply the EBM training objective to other baseline methods? And finally what is the the best architecture for label conditioning that causes the minimum interference with old data? To answer these questions, we first report experiments on the *boundary-aware* setting in Section 5.1. In Section 5.2, we then show that EBMs can also be applied to the *boundary-agnostic* setting.

5.1 EXPERIMENTS ON BOUNDARY-AWARE SETTING

5.1.1 Datasets and evalution protocols

Datasets. We evaluate the proposed EBMs on the split MNIST (Zenke et al., 2017), permuted MNIST (Kirkpatrick et al., 2017), CIFAR-10 (Krizhevsky et al., 2009), and CIFAR-100 (Krizhevsky et al., 2009) datasets. The split MNIST dataset is obtained by splitting the original MNIST dataset (LeCun et al., 1998) into 5 tasks with each task having 2 classes. This dataset has 60,000 training images and 10,000 test images. The permuted MNIST protocol has 10 tasks, each task with 10 classes. For each task, the original images pixels are randomly permuted to generate 32×32 images. We separate CIFAR-10 into 5 tasks, each task with 2 classes. Similarly, CIFAR-100 is split into 10

Table 1: Evaluation of class-incremental learning on the *boundary-aware* setting. Test accuracy on four datasets is reported. Each experiment is performed at least 10 times with different random seeds, the results are reported as the mean \pm SEM over these runs. Note our comparison is restricted to methods that do not replay stored or generated data.

Method	splitMNIST	permMNIST	CIFAR-10	CIFAR-100
SBC	19.90 ± 0.02	17.26 ± 0.19	19.06 ± 0.01	8.18 ± 0.10
EWC	20.01 ± 0.06	25.04 ± 0.50	18.99 ± 0.01	8.20 ± 0.09
Online EWC	19.96 ± 0.07	33.88 ± 0.49	19.07 ± 0.01	8.38 ± 0.15
SI	19.99 ± 0.06	29.31 ± 0.62	19.14 ± 0.02	9.24 ± 0.22
LwF	23.85 ± 0.44	22.64 ± 0.23	19.20 ± 0.30	10.71 ± 0.11
MAS	19.50 ± 0.30	-	20.25 ± 1.54	8.44 ± 0.27
BGD	19.64 ± 0.03	84.78 ± 1.30	-	-
EBM	$\textbf{53.12} \pm \textbf{0.04}$	$\textbf{87.78} \pm \textbf{0.01}$	$\textbf{40.19} \pm \textbf{0.01}$	$\textbf{30.28} \pm \textbf{0.28}$

tasks with each task having 10 classes. These last two datasets each have 50,000 training images and 10,000 test images.

Evaluation protocols. As noted by van de Ven & Tolias (2019), the above task protocols could be evaluated according either the task-incremental, domain-incremental, or class-incremental learning scenario. Most CL approaches perform fairly good on the first two simpler scenarios, but fail when asked to do class-incremental learning, which is considered as the most natural and also the hardest setting for continual learning (Tao et al., 2020a; He et al., 2018; Tao et al., 2020b). In this paper, we perform all experiments according to the class-incremental learning scenario.

5.1.2 Comparisons with existing methods

Successful existing methods for class-incremental learning either rely on an external quota of memory (Rebuffi et al., 2017; Hayes et al., 2020) or on using generative replay (Shin et al., 2017; van de Ven et al., 2020). A disadvantage of these methods is that they are relatively expensive in terms of memory and/or computation. In this paper, we focus on continual learning without using replay and without storing data.

We compare our proposed EBM method with available baseline models that do not use replay, including the standard softmax-based classifier (SBC), EWC (Kirkpatrick et al., 2017), Online EWC (Schwarz et al., 2018), c (Zenke et al., 2017), LwF (Li & Hoiem, 2017), MAS (Aljundi et al., 2019), and BGD (Zeno et al., 2018). The class-incremental learning results on four datasets are shown in Table 1. For SBC, EWC, Online EWC, Online EWC, LwF on splitMNIST, permuted MNIST, and CIFAR-100, we use the results reported in (van de Ven & Tolias, 2019; van de Ven et al., 2020). For BGD, we use the results reported in the original paper (Zeno et al., 2018). For MAS, we use the result from (Prabhu et al., 2020; Zhang et al., 2020). We performed the other experiments ourselves using the public available code.

All the baselines and EBMs use similar model architectures. For split MNIST and permuted MNIST we use several fully-connected layers, and for CIFAR-10 and CIFAR-100 we use a convolutional network (see Appendix B for details). For CIFAR-100, all compared models used convolutional layers that were pre-trained on CIFAR-10. Each experiment was performed at least 10 times with different random seeds, with results reported as the mean \pm SEM. Similar training regimes were used for the EBMs and baselines. On the split MNIST, permuted MNIST, and CIFAR-10 datasets, we trained for 2000 iterations per task. On the CIFAR-100 dataset we trained for 5000 iterations per task. For all experiments, we used the adam optimizer with learning rate $1e^{-4}$.

As shown in Table 1, EBMs have a significant improvement over the baseline methods on all the datasets, showing that EBMs forget less when updating models for new tasks.

5.1.3 QUALITATIVE ANALYSIS

Energy landscape. To better understand why EBMs suffer less from catastrophic forgetting than standard softmax-based classifiers, we qualitatively compare the change in energy landscapes of both methods as the learning progresses. In Figure 2, we show the energy landscapes after training on task 9 and task 10 of the permuted MNIST dataset. For the softmax-based classifier (SBC), the energy for each class is given by the negative of the predicted probability for that class. Each datapoint has 100 energy values (EBM) or probabilities (SBC) corresponding to the 100 labels in

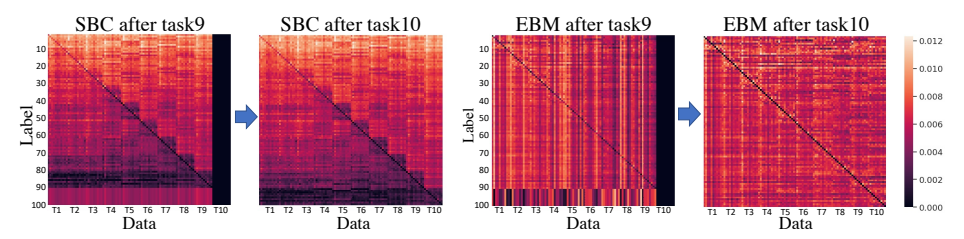


Figure 2: Energy landmaps of SBC and EBMs after training on task T_9 and T_{10} on permuted MNIST. The darker the diagonal is, the better the model is in preventing forgetting previous tasks.

the dataset, and for each datapoint these values are normalized over all 100 classes. Dark elements on the diagonal indicate correct model predictions. After training on task T_9 , SBC assigns high probabilities to classes from task T_9 (80-90) for almost all the data from task T_1 to T_9 . After learning task T_{10} , the highest probabilities shift to classes from task T_{10} (90-100). The standard classifier thus tends to assign high probabilities to new classes for both old and new data, indicating forgetting. On the other hand, the EBM has low energies across the diagonal, which means that after training on new tasks, EBM still assigns low energies to the true labels of data from previously tasks. This shows that EBM is better than SBC at learning new tasks without catastrophically forgetting of old tasks.

Predicted class distribution. In Figure 3, for the splitMNIST dataset, we plot the proportional distribution of predicted classes. Only data from the tasks seen so far was used for this figure. Taking the second panel in the first row as an example, it shows the distribution of predicted labels on test data from the first two tasks after finishing training on the second task. This means that so far the model has seen four classes: {1,2,3,4}. Since the number of test images from each class are similar, the ground truth proportional distribution should be uniform over those four classes. After training on the first task, the predictions of SBC are



Figure 3: Predicted label distribution after learning each task on the split MNIST dataset. The SBC only predicts classes from the current task, while our EBM predicts classes for all seen classes.

indeed roughly uniformly distributed over the first two classes (first panel). However, after learning new tasks, SBC only predicts classes from the most recent task, indicating that SBC failed to correctly memorize classes from previously seen tasks. On the other hand, the predictions of EBM are substantially more uniformly distributed over all classes seen so far.

In the Appendix, we provide further analyses comparing the continual learning behavior of SBC and EBMs, including testing accuracy curves throughout training in Appendix A.1, confusion matrices in Appendix A.2, an analysis of model capacity in Appendix A.3, a comparison of parameter importance in Appendix A.4, and an evaluation of the ability of proposed EBMs in preventing interference with past data when learning classification on new classes in Appendix A.5.

5.1.4 IS THE STRONG PERFORMANCE OF EBMS DUE TO THE ENERGY TRAINING OBJECTIVE OR DUE TO THE LABEL CONDITIONING?

Effect of energy training objective. We conduct an experiment on the CIFAR-100 dataset to investigate how different training objectives influence the CL results of the EBM. In Table 2, we compare three different strategies for selecting the set of negative samples $\mathcal N$. The first strategy uses all seen classes so far as negative labels (All Neg Seen), which is most similar to the way that the traditional feed-forward classifier is optimized. The second one takes all the classes in the current batch as negative labels (All Neg Batch). The last one randomly selects

Table 2: Performance of EBM on CIFAR-100 with different strategies for selecting the negative samples.

Dataset	CIFAR-100
All Neg Seen	8.07 ± 0.10
All Neg Batch	29.03 ± 0.53
1 Neg Batch	30.28 ± 0.28

one class from the current batch as the negative as we reported in Section 4.3.1 (1 Neg Batch). Note that the negative labels do not include the ground truth class in all these three strategies. We found using only one negative sample generates the best result, and using negatives sampled from classes in the current batch is better than from all seen classes. Since the loss in Equation 6 aims

Table 3: Results of baselines using our training objective and their original one.

	split MNIST		CIFAR-10	
	Original	Ours	Original	Ours
SBC	19.90 ± 0.02	44.98 ± 0.05	19.06 ± 0.01	19.22 ± 0.02
EWC	20.01 ± 0.06	50.68 ± 0.04	18.99 ± 0.01	36.51 ± 0.03
Online EWC	19.96 ± 0.07	50.99 ± 0.03	19.07 ± 0.01	36.16 ± 0.02
SI	19.99 ± 0.06	49.44 ± 0.03	19.14 ± 0.02	35.12 ± 0.02
EBM	-	$\textbf{53.12} \pm \textbf{0.04}$	-	$\textbf{40.19} \pm \textbf{0.01}$

at improving the energy of negative samples while decreasing the energy of positive ones, sampling negatives from the current batch has less interference with previous classes than sampling from all seen classes. Using a single negative causes the minimum suppression on negative samples and thus has the best result.

Effect of label conditioning. Next, we test whether the label conditioning in our EBMs is important for their performance. We test this by modifying the training objective of baseline models to that of our proposed energy objective, which is the same as running our EBMs without the label conditioning. The results of this comparison are listed in Table 3. The new training objective does not suppress the probability of old classes when improving the probability of new classes and thus achieves better results. However, EBMs still outperform the baselines, implying that the label conditioning architecture also contributes to why EBMs suffer less from catastrophic forgetting. We also show the testing accuracy curve in Appendix A.1.

To summarize, we showed that the strong performance of our EBMs is due to both the energy training objective and the label conditioning. Moreover, these results indicate that surprisingly, and counterintuitively, directly optimizing the cross-entropy loss used by existing approaches may not be the best way for continual learning.

5.1.5 Comparison of different energy network architectures

EBMs allow flexibility in integrating data information and label information in the energy function. To investigate where and how to combine the information from data ${\bf x}$ and label y, we conduct a series of experiments on the CIFAR-10 dataset. Table 4 shows four model architectures (V1-V4) that combine ${\bf x}$ and y in the early, middle, and late stages, respectively (see Appendix B for the architecture details). We find combining ${\bf x}$ and y in the late stage (V4) performs the best. We note that instead of learning a feature embedding of label y, we can use a fixed projection matrix which is randomly sampled from the uniform distribution $\mathcal{U}(0,1)$. Even using this fixed random projection can already generates better results than most baselines in Table 1. Note further

Table 4: Performance of EBM on CIFAR-10 with different label conditioning architectures.

Dataset	CIFAR-10
Beginning (V1)	13.69 ± 0.02
Middle(V2)	20.16 ± 0.02
Middle(V3)	18.36 ± 0.02
End (V4)	38.13 ± 0.01
End Fix (V4)	34.30 ± 0.03
End Fix Norm2 (V4)	33.91 ± 0.02
End Fix Softmax (V4)	35.97 ± 0.01
End Norm2 (V4)	37.23 ± 0.02
End Softmax (V4)	$\textbf{40.19} \pm \textbf{0.01}$

that the number of trainable parameters in the "Fix" setting is much lower than that of the baselines. Using a learned feature embedding of y can further improve the result. We may also apply different normalization methods over the feature channel of y. We find that Softmax (**End Softmax (V4)**) is better than the L2 normalization (**End Norm2 (V4)**) and no normalization (**End (V4)**).

5.1.6 SPLIT CIFAR-100 WITH DIFFERENT NUMBERS OF TASKS

To test the generality of our proposed EBMs, in Table 5 we repeat the boundary-aware experiments on CIFAR-100 for different number of classes per task. In Table 1, the CIFAR-100 dataset was split up into 10 tasks, resulting in 10 classes per task. Here we additionally split CIFAR-100 up into 5 tasks (i.e., 20 classes per task), 20 tasks (i.e., 5 classes per task) and 50 tasks (i.e., 2 classes per task). For all settings, we find that our EBM substantially outperforms the baselines.

5.2 EXPERIMENTS ON BOUNDARY-AGNOSTIC SETTING

When applying continual learning in real life, boundaries are not usually well defined between different tasks. Most existing continual learning methods are often tailored to the problem setup

Table 5: Comparison of our EBM with baselines on different variants of the split CIFAR-100 protocol. Shown is the class-incremental learning performance on the *boundary-aware* setting after all tasks have been learned. Each experiment is run 10 times with different random seeds, results are reported as mean \pm SEM.

Method		CIFAR-100		
Method	5 tasks	10 tasks	20 tasks	50 tasks
SBC	14.74 ± 0.20	8.18 ± 0.10	4.46 ± 0.03	1.91 ± 0.02
EWC	14.78 ± 0.21	8.20 ± 0.09	4.46 ± 0.03	1.91 ± 0.02
SI	14.07 ± 0.24	9.24 ± 0.22	4.37 ± 0.04	1.88 ± 0.03
LwF	25.75 ± 0.14	10.71 ± 0.11	12.18 ± 0.16	7.68 ± 0.16
EBM	$\textbf{34.88} \pm \textbf{0.14}$	$\textbf{30.28} \pm \textbf{0.28}$	$\textbf{25.04} \pm \textbf{0.33}$	$\textbf{13.60} \pm \textbf{0.50}$

Table 6: Evaluation of class-incremental learning performance on the *boundary-agnostic* setting. Each experiment is performed 5 times with different random seeds, average test accuracy is reported as the mean \pm SEM over these runs. Note that our comparison is restricted to methods that do not replay stored or generated data.

Method	splitMNIST	permMNIST	CIFAR-10	CIFAR-100
SBC	24.03 ± 0.01	21.42 ± 0.01	23.30 ± 0.01	9.85 ± 0.02
Online EWC	39.62 ± 0.04	41.37 ± 0.04	22.53 ± 0.01	9.57 ± 0.02
SI	28.79 ± 0.01	35.71 ± 0.01	26.26 ± 0.01	10.42 ± 0.01
BGD	21.65 ± 0.02	26.15 ± 0.02	17.03 ± 0.01	8.50 ± 0.02
EBM	$\textbf{81.78} \pm \textbf{0.06}$	$\textbf{92.35} \pm \textbf{0.01}$	$\textbf{49.47} \pm \textbf{0.03}$	34.39 ± 0.24

where a fixed boundary between tasks is defined, and must be informed when the tasks are switched during training. We show that EBMs are able to flexibly perform continual learning across different problem setups, and perform well on the *boundary-agnostic* setting as well.

5.2.1 Datasets and evalution protocols

For the *boundary-agnostic* setting, we again use the same four datasets as above. We use the code of "continuous task-agnostic learning" proposed by (Zeno et al., 2018) to generate the training data stream. The transition between tasks goes slowly over time using a sampling function based on the probability of each task. There is a mixture of data from two different tasks during the transition and the proportion of new data gradually increases. All experiments are performed according to the class-incremental learning scenario.

5.2.2 Comparison with existing methods

We again focus on the investigation of the performance of different model architectures with similar model size and memory footprint, and we thus do no compare with replay-based methods. Since there is no knowledge on the number of tasks, previous methods of continual learning that rely on task boundaries are generally inapplicable. One trivial adaptation is to take the core action after every batch step instead of every task. However, doing such adaptation is impractical for most algorithms, such as EWC, because of the large computational complexity. However, we managed to run the Online EWC, SI, and BGD baselines in this way. All compared methods used similar model architectures as in the *boundary-aware* setting. Each experiment was performed 5 times with different random seeds, the results are reported as the mean \pm SEM over these runs.

The results are shown in Table 6. We observe that EBMs have a significant improvement on all the datasets. The experiments show that EBMs have good generalization ability for different continual learning problems as EBMs can naturally handle data streams with and without task boundaries.

6 Conclusion

In this paper, we show that energy-based models (EBMs) are a promising class of models in a variety of different continual learning settings. We demonstrate that EBMs exhibit many desirable characteristics to prevent catastrophic forgetting in continual learning, and we experimentally show that EBMs obtain strong performance on the challenging class-incremental learning scenario on multiple benchmarks, both in the boundary-aware and in the boundary-agnostic setting.

ACKNOWLEDGEMENTS

This work has been partly supported by the Lifelong Learning Machines (L2M) program of the Defence Advanced Research Projects Agency (DARPA) via contract number HR0011-18-2-0025.

REFERENCES

- Rahaf Aljundi, Klaas Kelchtermans, and Tinne Tuytelaars. Task-free continual learning. In *Proceedings of the IEEE Conference on Computer Vision and Pattern Recognition*, pp. 11254–11263, 2019.
- Sergey Bartunov, Jack W Rae, Simon Osindero, and Timothy P Lillicrap. Meta-learning deep energy-based memory models. *arXiv preprint arXiv:1910.02720*, 2019.
- David Belanger and Andrew McCallum. Structured prediction energy networks. In *International Conference on Machine Learning*, pp. 983–992, 2016.
- Yuntian Deng, Anton Bakhtin, Myle Ott, Arthur Szlam, and Marc'Aurelio Ranzato. Residual energy-based models for text generation. *arXiv preprint arXiv:2004.11714*, 2020.
- Yilun Du, Toru Lin, and Igor Mordatch. Model based planning with energy based models. *arXiv* preprint arXiv:1909.06878, 2019.
- Yilun Du, Shuang Li, and Igor Mordatch. Compositional visual generation and inference with energy based models. *arXiv preprint arXiv:2004.06030*, 2020.
- Sebastian Farquhar and Yarin Gal. Towards robust evaluations of continual learning. *arXiv preprint arXiv:1805.09733*, 2018.
- Chrisantha Fernando, Dylan Banarse, Charles Blundell, Yori Zwols, David Ha, Andrei A Rusu, Alexander Pritzel, and Daan Wierstra. Pathnet: Evolution channels gradient descent in super neural networks. *arXiv preprint arXiv:1701.08734*, 2017.
- Will Grathwohl, Kuan-Chieh Wang, Jörn-Henrik Jacobsen, David Duvenaud, Mohammad Norouzi, and Kevin Swersky. Your classifier is secretly an energy based model and you should treat it like one. *arXiv preprint arXiv:1912.03263*, 2019.
- Fredrik K Gustafsson, Martin Danelljan, Goutam Bhat, and Thomas B Schön. Energy-based models for deep probabilistic regression. In *Proceedings of the European Conference on Computer Vision (ECCV)*, 2020.
- Michael Gygli, Mohammad Norouzi, and Anelia Angelova. Deep value networks learn to evaluate and iteratively refine structured outputs. *arXiv preprint arXiv:1703.04363*, 2017.
- Tuomas Haarnoja, Haoran Tang, Pieter Abbeel, and Sergey Levine. Reinforcement learning with deep energy-based policies. *arXiv preprint arXiv:1702.08165*, 2017.
- Tyler L Hayes, Kushal Kafle, Robik Shrestha, Manoj Acharya, and Christopher Kanan. Remind your neural network to prevent catastrophic forgetting. In *European Conference on Computer Vision*, pp. 466–483. Springer, 2020.
- Chen He, Ruiping Wang, Shiguang Shan, and Xilin Chen. Exemplar-supported generative reproduction for class incremental learning. In *BMVC*, pp. 98, 2018.
- Kaiming He, Xiangyu Zhang, Shaoqing Ren, and Jian Sun. Deep residual learning for image recognition. In *Proceedings of the IEEE conference on computer vision and pattern recognition*, pp. 770–778, 2016.
- Geoffrey E Hinton. Training products of experts by minimizing contrastive divergence. *Neural computation*, 14(8):1771–1800, 2002.
- Saihui Hou, Xinyu Pan, Chen Change Loy, Zilei Wang, and Dahua Lin. Learning a unified classifier incrementally via rebalancing. In *Proceedings of the IEEE Conference on Computer Vision and Pattern Recognition*, pp. 831–839, 2019.

- Wenpeng Hu, Zhou Lin, Bing Liu, Chongyang Tao, Zhengwei Tao, Jinwen Ma, Dongyan Zhao, and Rui Yan. Overcoming catastrophic forgetting for continual learning via model adaptation. In *International Conference on Learning Representations*, 2019.
- John Ingraham, Adam J Riesselman, Chris Sander, and Debora S Marks. Learning protein structure with a differentiable simulator. In *ICLR*, 2019.
- James Kirkpatrick, Razvan Pascanu, Neil Rabinowitz, Joel Veness, Guillaume Desjardins, Andrei A Rusu, Kieran Milan, John Quan, Tiago Ramalho, Agnieszka Grabska-Barwinska, et al. Overcoming catastrophic forgetting in neural networks. *Proceedings of the national academy of sciences*, 114(13):3521–3526, 2017.
- Alex Krizhevsky, Geoffrey Hinton, et al. Learning multiple layers of features from tiny images. 2009.
- Yann LeCun, Corinna Cortes, and Christopher JC Burges. The mnist database of handwritten digits, 1998. *URL http://yann. lecun. com/exdb/mnist*, 10:34, 1998.
- Yann LeCun, Sumit Chopra, Raia Hadsell, M Ranzato, and F Huang. A tutorial on energy-based learning. Predicting structured data, 1(0), 2006.
- Timothée Lesort, Hugo Caselles-Dupré, Michael Garcia-Ortiz, Andrei Stoian, and David Filliat. Generative models from the perspective of continual learning. In 2019 International Joint Conference on Neural Networks (IJCNN), pp. 1–8. IEEE, 2019.
- Zhizhong Li and Derek Hoiem. Learning without forgetting. *IEEE transactions on pattern analysis and machine intelligence*, 40(12):2935–2947, 2017.
- David Lopez-Paz and Marc' Aurelio Ranzato. Gradient episodic memory for continual learning. In *Advances in Neural Information Processing Systems*, pp. 6467–6476, 2017.
- Davide Maltoni and Vincenzo Lomonaco. Continuous learning in single-incremental-task scenarios. *Neural Networks*, 116:56–73, 2019.
- Nicolas Y Masse, Gregory D Grant, and David J Freedman. Alleviating catastrophic forgetting using context-dependent gating and synaptic stabilization. *Proceedings of the National Academy of Sciences*, 115(44):E10467–E10475, 2018.
- Martin Mundt, Yong Won Hong, Iuliia Pliushch, and Visvanathan Ramesh. A wholistic view of continual learning with deep neural networks: Forgotten lessons and the bridge to active and open world learning. *arXiv* preprint arXiv:2009.01797, 2020.
- German I Parisi, Ronald Kemker, Jose L Part, Christopher Kanan, and Stefan Wermter. Continual lifelong learning with neural networks: A review. *Neural Networks*, 2019.
- Tetiana Parshakova, Jean-Marc Andreoli, and Marc Dymetman. Distributional reinforcement learning for energy-based sequential models. *arXiv preprint arXiv:1912.08517*, 2019.
- Ameya Prabhu, Philip HS Torr, and Puneet K Dokania. Gdumb: A simple approach that questions our progress in continual learning. 2020.
- Jathushan Rajasegaran, Munawar Hayat, Salman H Khan, Fahad Shahbaz Khan, and Ling Shao. Random path selection for continual learning. In *Advances in Neural Information Processing Systems*, pp. 12669–12679, 2019.
- Jathushan Rajasegaran, Salman Khan, Munawar Hayat, Fahad Shahbaz Khan, and Mubarak Shah. itaml: An incremental task-agnostic meta-learning approach. In *Proceedings of the IEEE/CVF Conference on Computer Vision and Pattern Recognition*, pp. 13588–13597, 2020.
- Sylvestre-Alvise Rebuffi, Alexander Kolesnikov, Georg Sperl, and Christoph H Lampert. icarl: Incremental classifier and representation learning. In *Proceedings of the IEEE conference on Computer Vision and Pattern Recognition*, pp. 2001–2010, 2017.
- Anthony Robins. Catastrophic forgetting, rehearsal and pseudorehearsal. *Connection Science*, 7(2): 123–146, 1995.

- Amirmohammad Rooshenas, Dongxu Zhang, Gopal Sharma, and Andrew McCallum. Search-guided, lightly-supervised training of structured prediction energy networks. In *Advances in Neural Information Processing Systems*, pp. 13522–13532, 2019.
- Andrei A Rusu, Neil C Rabinowitz, Guillaume Desjardins, Hubert Soyer, James Kirkpatrick, Koray Kavukcuoglu, Razvan Pascanu, and Raia Hadsell. Progressive neural networks. arXiv preprint arXiv:1606.04671, 2016.
- Ruslan Salakhutdinov and Geoffrey Hinton. Deep boltzmann machines. In David van Dyk and Max Welling (eds.), *Proceedings of the Twelth International Conference on Artificial Intelligence and Statistics*, volume 5 of *Proceedings of Machine Learning Research*, pp. 448–455, Hilton Clearwater Beach Resort, Clearwater Beach, Florida USA, 16–18 Apr 2009. PMLR. URL http://proceedings.mlr.press/v5/salakhutdinov09a.html.
- Benjamin Scellier and Yoshua Bengio. Equilibrium propagation: Bridging the gap between energy-based models and backpropagation. *Frontiers in computational neuroscience*, 11:24, 2017.
- Jonathan Schwarz, Jelena Luketina, Wojciech M Czarnecki, Agnieszka Grabska-Barwinska, Yee Whye Teh, Razvan Pascanu, and Raia Hadsell. Progress & compress: A scalable framework for continual learning. arXiv preprint arXiv:1805.06370, 2018.
- Joan Serra, Didac Suris, Marius Miron, and Alexandros Karatzoglou. Overcoming catastrophic forgetting with hard attention to the task. *arXiv preprint arXiv:1801.01423*, 2018.
- Hanul Shin, Jung Kwon Lee, Jaehong Kim, and Jiwon Kim. Continual learning with deep generative replay. In *Advances in Neural Information Processing Systems*, pp. 2990–2999, 2017.
- Karen Simonyan and Andrew Zisserman. Very deep convolutional networks for large-scale image recognition. *arXiv preprint arXiv:1409.1556*, 2014.
- Christian Szegedy, Wei Liu, Yangqing Jia, Pierre Sermanet, Scott Reed, Dragomir Anguelov, Dumitru Erhan, Vincent Vanhoucke, and Andrew Rabinovich. Going deeper with convolutions. In *Proceedings of the IEEE conference on computer vision and pattern recognition*, pp. 1–9, 2015.
- Xiaoyu Tao, Xinyuan Chang, Xiaopeng Hong, Xing Wei, and Yihong Gong. Topology-preserving class-incremental learning. 2020a.
- Xiaoyu Tao, Xiaopeng Hong, Xinyuan Chang, Songlin Dong, Xing Wei, and Yihong Gong. Few-shot class-incremental learning. In *Proceedings of the IEEE/CVF Conference on Computer Vision and Pattern Recognition*, pp. 12183–12192, 2020b.
- Lifu Tu and Kevin Gimpel. Benchmarking approximate inference methods for neural structured prediction. *arXiv preprint arXiv:1904.01138*, 2019.
- Lifu Tu, Richard Yuanzhe Pang, Sam Wiseman, and Kevin Gimpel. Engine: Energy-based inference networks for non-autoregressive machine translation. *arXiv preprint arXiv:2005.00850*, 2020.
- Gido M van de Ven and Andreas S Tolias. Three scenarios for continual learning. *arXiv preprint arXiv:1904.07734*, 2019.
- Gido M van de Ven, Hava T Siegelmann, and Andreas S Tolias. Brain-inspired replay for continual learning with artificial neural networks. *Nature Communications*, 11:4069, 2020.
- Yue Wu, Yinpeng Chen, Lijuan Wang, Yuancheng Ye, Zicheng Liu, Yandong Guo, and Yun Fu. Large scale incremental learning. In *Proceedings of the IEEE Conference on Computer Vision and Pattern Recognition*, pp. 374–382, 2019.
- Jianwen Xie, Yang Lu, Song-Chun Zhu, and Yingnian Wu. A theory of generative convnet. In *International Conference on Machine Learning*, pp. 2635–2644, 2016.
- Jianwen Xie, Yang Lu, Ruiqi Gao, Song-Chun Zhu, and Ying Nian Wu. Cooperative training of descriptor and generator networks. *IEEE transactions on pattern analysis and machine intelligence*, 42(1):27–45, 2018.

- Kelvin Xu, Jimmy Ba, Ryan Kiros, Kyunghyun Cho, Aaron Courville, Ruslan Salakhudinov, Rich Zemel, and Yoshua Bengio. Show, attend and tell: Neural image caption generation with visual attention. In *International conference on machine learning*, pp. 2048–2057, 2015.
- Jaehong Yoon, Eunho Yang, Jeongtae Lee, and Sung Ju Hwang. Lifelong learning with dynamically expandable networks. *arXiv preprint arXiv:1708.01547*, 2017.
- Guanxiong Zeng, Yang Chen, Bo Cui, and Shan Yu. Continual learning of context-dependent processing in neural networks. *Nature Machine Intelligence*, 1(8):364–372, 2019.
- Friedemann Zenke, Ben Poole, and Surya Ganguli. Continual learning through synaptic intelligence. In *Proceedings of the 34th International Conference on Machine Learning-Volume 70*, pp. 3987–3995. JMLR. org, 2017.
- Chen Zeno, Itay Golan, Elad Hoffer, and Daniel Soudry. Task agnostic continual learning using online variational bayes. *arXiv preprint arXiv:1803.10123*, 2018.
- Song Zhang, Gehui Shen, and Zhi-Hong Deng. Self-supervised learning aided class-incremental lifelong learning. *arXiv preprint arXiv:2006.05882*, 2020.

A ADDITIONAL ANALYSES

Extending the results presented in Section 5.1, here we further compare EBMs with the baseline models by providing additional quantitative analyses of their performance. We show testing accuracy curves in Section A.1, confusion matrices between the ground truth labels and model predictions in Section A.2, model capacity comparisons in Section A.3, and parameter importance measurement in Section A.4. In Section A.5, we provide more details of the label conditioning analysis mentioned in Section 5.1.4.

A.1 TESTING ACCURACY CURVE

In Section 5.1.4, we show that the proposed EBM training objective is also applicable to baseline approaches and improves their performance significantly on the *Class-IL* setting. Figure 4 shows the testing accuracy of each task as the training progresses. We compare the standard classifier (SBC), classifier using our training objective (SBC*), and our EBMs. The left figures show results on the split MNIST dataset while the right figures show results on the permuted MNIST dataset. We observe that the accuracy of old tasks in SBC drop sharply when learning new tasks, while the EBM training objective can mitigate the forgetting problem. The curve on EBMs drops even slower than SBC and SBC*, implying the proposed energy objective can mitigate the catastrophic forgetting problem.

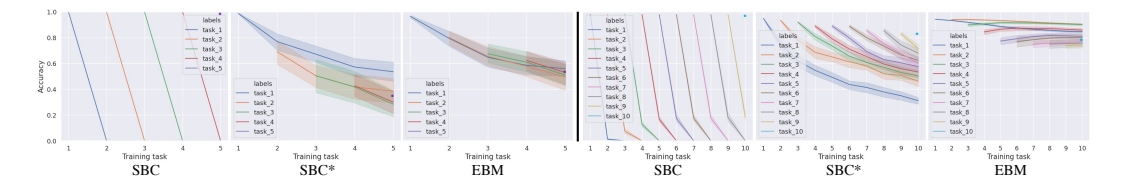


Figure 4: Class-IL testing accuracy of the standard classifier (SBC), classifier using our training objective (SBC*), and EBMs on each task on the split MNIST dataset (left) and permuted MNIST dataset (right).

A.2 CLASS CONFUSION MATRIX AT THE END OF LEARNING

Here, we show confusion matrices for EBM and SBC. A confusion matrix illustrates the relationship between the ground truth labels and the predicted labels. Figure 5 shows the confusion matrices after training on all the tasks on the split MNIST dataset and permuted MNIST dataset. The standard classifier tends to only predict the classes from the last task (class 8, 9 for split MNIST and classes 90-100 for permuted MNIST). The EBMs on the other hand have high values along the diagonal, which indicates that the predicted results match the ground truth labels for all the sequentially learned tasks.

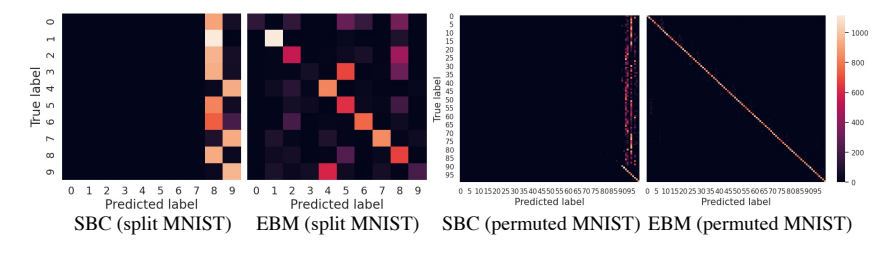


Figure 5: Confusion matrices between ground truth labels and predicted labels at the end of learning on split MNIST (left) and permuted MNIST (right). The lighter the diagonal is, the more accurate the predictions are.

A.3 MODEL CAPACITY

Another hypothesized reason for why EBMs suffer less from catastrophic forgetting than standard classifiers is potentially their larger effective capacity. To analyze effective capacity of our models, we test the model capacity of the standard classifier and EBMs on both the generated images and natural images.

Model capacity on generated images. We generate a large randomized dataset of 32×32 images with each pixel value uniformly sampled from -1 to 1. Each image is then assigned a random class label between 0 and 10. We measure the model capacity by evaluating to what extent the model can fit a such dataset. For both the standard classifier and the EBM, we evaluate three different sizes of models (small, medium, and large). For a fair comparison, we control the EBM and classifier have similar number of parameters. The Small EBM and SBC have 2,348,545 and 2,349,032 parameters respectively. The medium models have 5,221,377 (EBM) and 5,221,352 (SBC) parameters while the large models have 33,468,417 (EBM) and 33,465,320 (SBC) parameters. We use the model architectures in Table 7a and Table 7b for EBMs and classifiers.

The resulting training accuracies are shown in Figure 6 with the number of data ranges from one to five millions. Given any number of datapoints, EBM obtains higher accuracy than the classifier, demonstrating that indeed EBM has larger capacity to memorize data given a similar number of parameters. The gap between EBM and SBC increases when the models become larger. The larger capacity of EBM potentially enables it to memorize more data and mitigate the forgetting problem.

Model capacity on natural images. We also compare classifiers and EBMs on natural images from CIFAR-10. Each image is assigned a random class label between 0 and 10. We use the same network architecture as in Table 7a and Table 7b, but with a hidden unit size of h=256. Since there are only 50,000 images on CIFAR-10, we use a small classifier and EBM and train them on the full dataset. After training 100000 iterations, the EBM obtains a top-1 prediction accuracy of 82.81, while the classifier is 42.19. We obtain the same conclusion that EBM has larger capacity to memorize data given a similar number of parameters.

Table 7: The model architectures used for the model capacity analysis. h are 512, 1024, and 4096 for the small, medium and large network, respectively.

(a) The architecture of the EBM

$x = FC(32 \times 32 \times 3, h) (x)$
x = ReLU(x)
y = Embedding (y)
x = x * y
x = ReLU(x)
out = FC(h, 1) (x)

(b) The architecture of the standard classifier..

$x = FC(32 \times 32 \times 3, h) (x)$
x = ReLU(x)
x = FC(h, h)(x)
x = ReLU(x)
out = $FC(h, 10)(x)$

A.4 PARAMETER IMPORTANCE

To further understand why EBMs suffer less from catastrophic forgetting than standard classifiers, we design an experiment to test the importance of model parameters on past data. Inspired by the elastic weight consolidation (EWC) (Kirkpatrick et al., 2017), we estimate the importance of parameters for each tasks using the diagonal elements of the Fisher information matrix (FIM) F. Let θ_i be the model parameters after training on task T_i . Given one of previous tasks T_j , j < i, we evaluate how important each parameter is for tasks T_j . The k^{th} diagonal of F is defined as the gradient on the EBM loss

$$F_{i,k} = \mathbb{E}_{\mathbf{x} \sim T_j} \left[\nabla_{\theta_{i,k}} \left(E_{\theta_i}(\mathbf{x}, y^+) + \log \sum_{y} \exp(-E_{\theta_i}(\mathbf{x}, y)) \right)^2 \right], \tag{10}$$

where \mathbf{x} is sampled from tasks T_j and $E(\mathbf{x}, y^+)$ is the energy value of the input data \mathbf{x} and ground truth label y^+ . $y \in Y_j$ are classes randomly selected from the current batch. Here we use a single

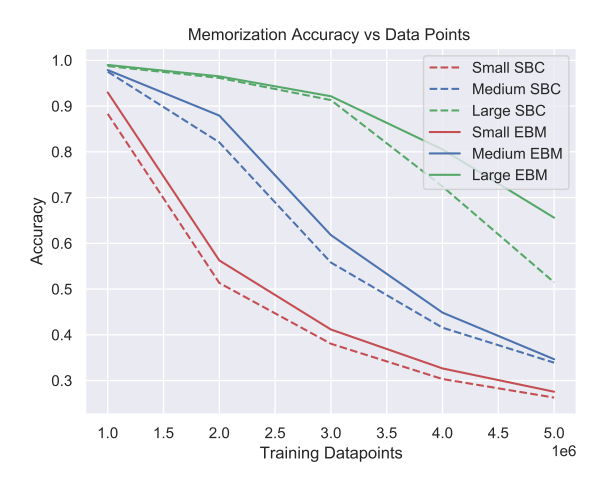


Figure 6: Model capacity of the standard classifier (SBC) and EBM using different model sizes.

negative class. The above equation assigns high values to parameters crucial to task T_j as their gradients with respect to the loss are larger. Since the diagonal elements of the fisher information matrix measure the importance of each parameter to a given task, the density of diagonal elements represents the proportion of important parameters over all parameters. More density means more parameters are important for the given task and less parameters can be recruited for new tasks. Ideally, we expect these values to be sparse.

In Figure 7, we show the diagonal elements of the standard classifier (SBC), classifier using our training objective (SBC*), and our EBMs on the split MNIST dataset. For SBC and SBC*, we follow (Kirkpatrick et al., 2017) to compute their fisher information matrices. For comparisons across multiple models, we normalize the FIM diagonal elements of each method to be between 0 and 1 and report the normalized results in Figure 7. For example, "Fisher 5 on data 1" shows the diagonal elements of the Fisher information matrix obtained by Equation 10 using the model parameters θ_5 (after training on task T_5) and data \mathbf{x}, y^+, y from task T_1 . The distribution of EBMs is sparser than SBC and SBC* indicating that EBMs have fewer important parameters for previous data. Updating parameters for the new task will have less negative impact on old tasks. In addition, more parameters can be used for learning new tasks if the distribution is sparse. This may provide another explanation for why EBMs can mitigate catastrophic forgetting.

A.5 INTERFERENCE WITH PAST DATA

In this part, we try to evaluate the ability of label conditioning in the proposed EBM in preventing interference with past data when learning classification on new classes. Formally, let \mathbf{x}_i and \mathbf{x}_j be two data points and θ_i be the model parameters after training on \mathbf{x}_i . The model parameters change $\Delta\theta(\mathbf{x}_j)$ after learning new data \mathbf{x}_j . We test the difference between the losses $\mathcal{L}_{ML}(\mathbf{x}_i \mid \theta_i)$ and $\mathcal{L}_{ML}(\mathbf{x}_i \mid \theta_i + \Delta\theta(\mathbf{x}_j))$. Ideally, we expect $\mathcal{L}_{ML}(\mathbf{x}_i \mid \theta_i + \Delta\theta(\mathbf{x}_j)) \leq \mathcal{L}_{ML}(\mathbf{x}_i \mid \theta_i)$ for $\mathbf{x}_i \neq \mathbf{x}_j$, which means the update on new data has no influence or positive influence on the old data. The first-order expansion gives

$$\mathcal{L}_{ML}(\mathbf{x}_i \mid \theta_i + \triangle \theta(\mathbf{x}_j)) \approx \mathcal{L}_{ML}(\mathbf{x}_i \mid \theta_i) + \nabla_{\theta_i} \mathcal{L}_{ML}(\mathbf{x}_i \mid \theta_i)^T \triangle \theta(\mathbf{x}_j). \tag{11}$$

To make our desired equality hold, the gradient at \mathbf{x}_i should be $\nabla_{\theta_i} \mathcal{L}_{ML}(\mathbf{x}_i \mid \theta_i)^T \triangle \theta(\mathbf{x}_j) \leq 0$. $\phi = \nabla_{\theta_i} \mathcal{L}_{ML}(\mathbf{x}_i \mid \theta_i)^T \triangle \theta(\mathbf{x}_j)$ can be used to measure the influence of updating models on new data on the performance of old data. The smaller the value is, the less negative influence on old data, and thus the better the model is in preventing forgetting.

We compare the proposed EBMs with the standard classifier (SBC) and SBC using our EBMs training objective (SBC*). We use the contrastive divergence loss in Equation 6 for EBM and cross-entropy loss for SBC and SBC* to get their ϕ . We obtain θ_i by training on 200 randomly selected data from task1 and compute its gradient after training. Then we perform a single step optimization on 200 data that are randomly selected from task2 and average their parameters to get θ_j . We

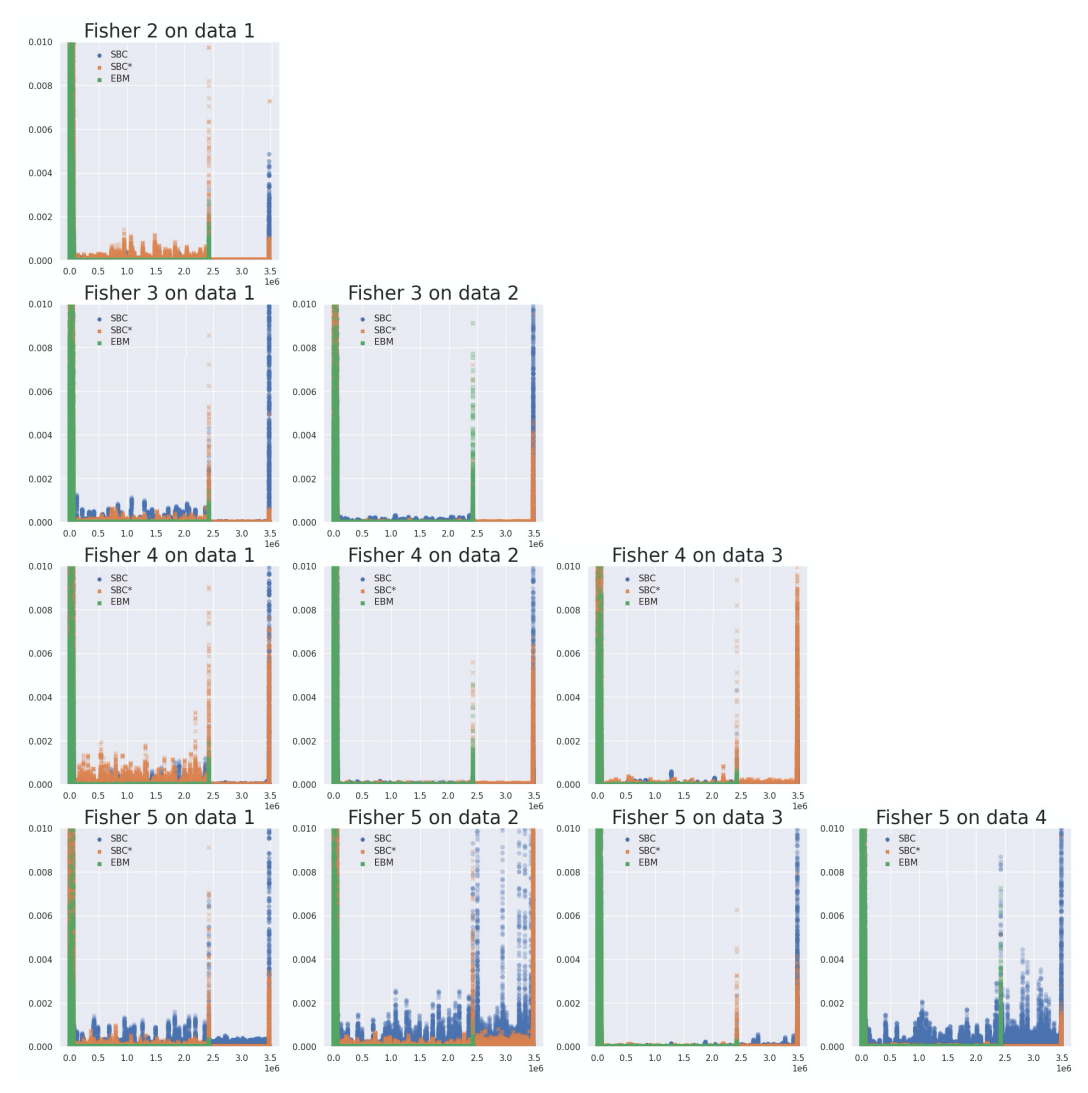


Figure 7: Parameter importance on different tasks. The x-axis represents each different parameter and y-axis is the FIM value in Equation 10. The sparser the parameters are, the fewer important parameters for previous data, which may contribute to why EBMs has less influence on previous tasks after training on new data. "Fisher 5 on data 1" means the diagonal elements of the fisher information matrix obtained by Equation 10 using the model parameters θ_5 (after training on task T_5) and data from task T_1 .

compute ϕ using the inner product of $\triangle \theta(\mathbf{x}_j) = \theta_j - \theta_i$ and the gradient $\nabla_{\theta_i} \mathcal{L}_{ML}(\mathbf{x}_i \mid \theta_i)$. For comparisons among multiple approaches, we normalize the ϕ of each method by dividing its maximum element value of θ_i and scale ϕ based on the length of θ , as SBC and EBMs have different number of parameters.

For results on split MNIST, the average value of ϕ over all tasks of SBC, SBC*, and EBMs are $\phi_{\rm SBC}=0.168,\,\phi_{\rm SBC^*}=0.004,\,$ and $\phi_{\rm EBM}=-3.743e^{-5},\,$ respectively. For CIFAR-10, the results are $\phi_{\rm SBC}=1.104,\,\phi_{\rm SBC^*}=0.043,\,$ and $\phi_{\rm EBM}=4.414e^{-5},\,$ respectively. We found EBMs have smaller ϕ than SBC and SBC*, which is consistent with our analysis that the conditional gain $g(\mathbf{y})$ serves as an attention filter that could select the relevant information between \mathbf{x} and \mathbf{y} and make parameter updates cause less interference with old data, which contributes to why EBMs suffer less from catastrophic forgetting.

B MODEL ARCHITECTURES

Here we provide details of the model architectures used on the different datasets.

Images from the split MNIST and permuted MNIST datasets are grey-scale images. The base-line models for these datasets, similar as in (van de Ven & Tolias, 2019), consist of several fully-connected layers. For the EBMs we use similar number of parameters. The model architectures of EBMs on the split MNIST dataset and permuted MNIST dataset are the same, but have different input and output dimensions and hidden sizes. The model architectures of EBMs and baseline models on the split MNIST dataset are shown in Table 8a and Table 8b respectively. The model architectures of EBMs and baseline models on the permuted MNIST dataset are shown in Table 9a and Table 9b.

Images from the CIFAR-10 and CIFAR-100 datasets are RGB images. For CIFAR-10, we use a small convolutional network for both the baseline models and the EBMs. The model architectures of EBMs on the CIFAR-10 dataset are shown in Table 10a, Table 10b, Table 10c, Table 10d, and Table 10e. We investigate different architectures to search for the effective label conditioning on EBMs training as described in Section 5.1.5. The baseline models on CIFAR-10 are given in Table 10f. The model architectures used on the CIFAR-100 dataset are detailed in Table 11.

Table 8: The model architectures used on split MNIST. h=400.

(a) The architecture of the EBMs.

x = FC(784, h)(x)
x = ReLU(x)
y = Embedding(y)
x = x * Norm2 (y) + x
x = ReLU(x)
out = FC(h, 1) (x)

(b) The architecture of the baseline models.

x = FC(784, h)(x)
x = ReLU(x)
x = FC(h, h)(x)
x = ReLU(x)
out = $FC(h, 10)(x)$

Table 9: The model architectures used on permuted MNIST. h = 1000.

(a) The architecture of the EBMs.

x = FC(1024, h)(x)
x = ReLU(x)
y = Embedding (y)
x = x * Norm2(y) + x
x = ReLU(x)
out = FC(h, 1)(x)

(b) The architecture of the baseline models.

x = FC(1024, h)(x)
x = ReLU(x)
x = FC(h, h)(x)
x = ReLU(x)
out = $FC(h, 100)(x)$

Table 10: The model architectures used on the CIFAR-10 dataset.

(a) EBM: Beginning (V1)	(b) EBM: Middle (V2)	(c) EBM: Middle (V3)
Input: x, y	Input: x, y	Input: x, y
y = Embedding(N, 3) (y)	$x = \text{Conv2d}(3 \times 3, 3, 32) (x)$	$x = \text{Conv2d}(3 \times 3, 3, 32) (x)$
y = Softmax(dim=-1)(y)	x = ReLU(x)	x = ReLU(x)
y = y * y.shape[-1]	$x = Conv2d(3 \times 3, 32, 32) (x)$	$x = \text{Conv2d}(3 \times 3, 32, 32) (x)$
x = x * y	x = ReLU(x)	x = ReLU(x)
$x = Conv2d(3 \times 3, 3, 32) (x)$	y = Embedding(N, 32) (y)	x = Maxpool(2, 2) (x)
x = ReLU(x)	y = Softmax(dim=-1)(y)	$x = \text{Conv2d}(3 \times 3, 32, 64) (x)$
$x = Conv2d(3 \times 3, 32, 32) (x)$	y = y * y.shape[-1]	x = ReLU(x)
x = ReLU(x)	x = x * y	$x = \text{Conv}2d(3 \times 3, 64, 64) (x)$
x = Maxpool(2, 2) (x)	x = Maxpool(2, 2) (x)	x = ReLU(x)
$x = Conv2d(3\times3, 32, 64) (x)$	$x = \text{Conv2d}(3 \times 3, 32, 64) (x)$	y = Embedding(N, 64) (y)
x = ReLU(x)	x = ReLU(x)	y = Softmax(dim=-1)(y)
$x = \text{Conv2d}(3 \times 3, 64, 64) (x)$	$x = \text{Conv2d}(3 \times 3, 64, 64) (x)$	y = y * y.shape[-1]
x = ReLU(x)	x = ReLU(x)	x = x * y
x = Maxpool(2, 2) (x)	x = Maxpool(2, 2) (x)	x = Maxpool(2, 2) (x)
x = FC(2304, 1024) (x)	x = FC(2304, 1024) (x)	x = FC(2304, 1024) (x)
x = ReLU(x)	x = ReLU(x)	x = ReLU(x)
out = $FC(1024, 1)(x)$	out = $FC(1024, 1)(x)$	out = $FC(1024, 1)(x)$
(d) EBM: End Fix Softmax (V4)	(e) EBM: End Softmax (V4)	(f) Baseline models
Input: x, y $x = Corr^{2}d(2x/2, 2, 2)(x)$	Input: x, y	Input: x
$x = \text{Conv2d}(3 \times 3, 3, 32) (x)$	$x = \text{Conv2d}(3 \times 3, 3, 32) (x)$	$x = \text{Conv2d}(3 \times 3, 3, 32) (x)$
x = ReLU(x)	x = ReLU(x)	x = ReLU(x)
$x = \text{Conv2d}(3 \times 3, 32, 32) (x)$	$x = \text{Conv2d}(3 \times 3, 32, 32) (x)$	$x = Conv2d(3 \times 3, 32, 32) (x)$
x = ReLU(x)	x = ReLU(x)	x = ReLU(x)
x = Maxpool(2, 2) (x)	x = Maxpool(2, 2) (x)	x = Maxpool(2, 2) (x)
$x = \text{Conv2d}(3 \times 3, 32, 64) (x)$	$x = \text{Conv2d}(3 \times 3, 32, 64) (x)$	$x = \text{Conv2d}(3 \times 3, 32, 64) (x)$
x = ReLU(x)	x = ReLU(x)	x = ReLU(x)
$x = \text{Conv2d}(3 \times 3, 64, 64) (x)$	$x = \text{Conv2d}(3 \times 3, 64, 64) (x)$	$x = \text{Conv2d}(3 \times 3, 64, 64) (x)$
x = ReLU(x)	x = ReLU(x)	x = ReLU(x)
x = Maxpool(2, 2) (x)	x = Maxpool(2, 2) (x)	x = Maxpool(2, 2) (x)
x = FC(2304, 1024) (x)	x = FC(2304, 1024) (x)	x = FC(2304, 1024) (x)
y = Random Projection (y)	y = Embedding(N, 1024) (y)	x = ReLU(x)
y = Softmax(dim=-1) (y)	y = Softmax(dim=-1) (y)	x = FC(1024, 1024) (x)
y = y * y.shape[-1]	y = y * y.shape[-1]	x = ReLU(x)
x = x * y	x = x * y	out = $FC(1024, 10) (x)$
out = $FC(1024, 1) (x)$	out = $FC(1024, 1)(x)$	<u> </u>

Table 11: The model architectures used on the CIFAR-100 dataset. Following van de Ven et al. (2020), for all models the convolutational layers were pre-trained on CIFAR-10. The 'BinaryMask'-operation fully gates a randomly selected subset of X% of the nodes, with a different subset for each y. Hyperparameter X was set using a gridsearch.

(a) The architecture of the EBMs.

Input: x, y
$x = Conv2d(3\times3, 3, 16) (x)$
x = BatchNorm(x)
x = ReLU(x)
$x = \text{Conv2d}(3 \times 3, 16, 32) (x)$
x = BatchNorm(x)
x = ReLU(x)
$x = \text{Conv2d}(3 \times 3, 32, 64) (x)$
x = BatchNorm(x)
x = ReLU(x)
$x = \text{Conv2d}(3 \times 3, 64, 128) (x)$
x = BatchNorm(x)
x = ReLU(x)
$x = \text{Conv2d}(3 \times 3, 128, 256) (x)$
x = FC(1024, 2000) (x)
x = ReLU(x)
x = BinaryMask(x, y)
x = FC(2000, 2000) (x)
x = ReLU(x)
x = BinaryMask(x, y)
out = $FC(2000, 1)(x)$

(b) The architecture of the baseline models.

Input: x
$x = Conv2d(3 \times 3, 3, 16) (x)$
x = BatchNorm(x)
x = ReLU(x)
$x = \text{Conv2d}(3 \times 3, 16, 32) (x)$
x = BatchNorm(x)
x = ReLU(x)
$x = \text{Conv2d}(3 \times 3, 32, 64) (x)$
x = BatchNorm(x)
x = ReLU(x)
$x = \text{Conv2d}(3 \times 3, 64, 128) (x)$
x = BatchNorm(x)
x = ReLU(x)
$x = \text{Conv2d}(3 \times 3, 128, 256) (x)$
x = FC(1024, 2000) (x)
x = ReLU(x)
x = FC(2000, 2000) (x)
x = ReLU(x)
out = $FC(2000, 100)(x)$